

Inelastic insights for molecular tunneling pathways: Bypassing the terminal groups†

Alessandro Troisi^{*a} and Mark A. Ratner^b

Received 14th February 2007, Accepted 28th February 2007

First published as an Advance Article on the web 21st March 2007

DOI: 10.1039/b702377d

As an example of the use of inelastic transport to deduce structure in molecular transport junctions, we compute the orientation dependence of the Inelastic Electron Tunneling (IET) spectrum of the 1-pentane monothiolate. We find that upon increasing the tilting angle of the molecule with respect to the normal to the electrode the spectrum changes as the intensity of some vibrations is enhanced. These differences occur because for higher tilting angles the tunneling path that bypasses the terminal group grows in importance. IETS can therefore be used to establish the molecular orientation in junctions terminating with alkyl chains and to investigate experimentally the relative importance of the available tunneling paths.

1. Introduction

One of the greatest problems that molecular electronics faced in the first ten years of development was the difficulty in characterizing the structure of molecular junctions, a problem directly related to the poor reproducibility of molecular electronics experiments.^{1,2} The application of Inelastic Electron Tunneling Spectroscopy (IETS)^{3,4} to molecular junctions provides a systematic and generally applicable method to characterize the junction as a working molecular device, with the advantage that the IET spectra are obtained from low-temperature current/voltage (I/V) measurements. In IETS, the second derivative of I with respect to V is plotted: peaks in this graph correspond to vibrational modes that are excited by the tunneling electrons. Ho measured IETS for the first time in single molecule junctions using an STM experimental set up (where, thanks to the STM image itself there is less need of structural information).⁵ The application to molecular wire junctions more strongly coupled to both electrodes was pioneered by the groups of Reed⁶ and Kushmerick.⁷ The high resolution of these first IETS spectra immediately suggested that information on the molecular junction can be extracted from these measurements. Unfortunately, the assignment/interpretation of these spectra is not easy and most of the information is bound to be of little use if the measurements are not associated with a predictive computational method. No rigorous selection rules are available and the correlation with the actual intensity pattern seen in other vibrational spectroscopies (Raman, IR) is only partial.

The first theoretical models for off-resonance inelastic tunneling focused on the process observed in a STM experimental setup and were based on an extension of the Tersoff–Hamman

formalism.^{8,9} To deal with the more general case of molecules strongly coupled to both electrodes, we proposed application of a Herzberg–Teller like vibronic expansion while describing the conductance as a scattering process.¹⁰ This approach led to simulated IET spectra in remarkable agreement with the experimental data of Kushmerick *et al.*¹¹ and allowed the interpretation of IETS spectra for hydrated junctions.¹² A similar expression for the inelastic conductance was obtained by Jiang *et al.*¹³ and by Paulsson *et al.*,¹⁴ who started respectively from a scattering formalism and from the non-equilibrium Green's function formalism (NEGF). In general the proposed formalisms are derived either from scattering theory¹⁵ or from NEGF,^{16–20} and certainly further work is necessary to clarify the relation between these derivations.

As for computation of the I/V characteristic in molecular junctions, for the simulation of IETS it is important to reach a balance between the accuracy of the theoretical method and the accuracy of the quantum chemical calculations that connect the theory with the experimental observables. The difficulties encountered in the simulation of IETS and I/V characteristics are quite different, so that the most appropriate approach for these two problems need not to be the same. IETS spectra are measured in the linear regime of the I/V curve, *i.e.* in the regime of off-(electronic) resonance tunneling and very low biases. Consequently, the precise position of the Fermi levels with respect to the molecular levels and the electrostatic potential drop across the junction are of minor importance in the IETS simulations (while they are crucial for the evaluation of the I/V characteristics). This explains why the simple formalism based on perturbation theory seems to give results as good as the non-perturbative approaches.²¹

IETS simulations require the calculation of molecular normal modes for a very complicated system usually made by a monolayer sandwiched between two electrodes, an unusual situation for normal mode analysis. Fortunately, molecular vibrations are very local in nature, so that the vibrations of the transporting molecules and the vibrations of the electrode atoms are separable 'to some extent'. Depending on the extent of separation several approximation schemes have been

^a Department of Chemistry and Centre of Scientific Computing, University of Warwick, Coventry, UK CV4 7AL. E-mail: a.troisi@warwick.ac.uk; Tel: +44 (0)2476 523228

^b Department of Chemistry, Center for Nanofabrication and Molecular Self-Assembly, Northwestern University, Evanston, Illinois 60208, USA

† The HTML version of this article has been enhanced with colour images.

proposed. It is possible to use the isolated molecule (perhaps with a few additional metal atoms) to compute the molecular normal modes, assuming that they are unchanged in the monolayer. The advantage of this approach is the wide experience in normal modes computation, using standard quantum chemical methods (e.g. 6-31G*/B3LYP), where standard scaling factors are used to bring the computed frequencies (for isolated molecules) within a few percent of the gas phase experimental values. Moreover, other vibrational spectroscopies on metal surfaces (EELS, SERS) have shown that the vibrational frequencies on the surface are generally very similar to those of the gas phase (except, of course, for the metal–molecule chemisorption bond). An alternative method is to consider two very large clusters containing many metal atoms to simulate the electrodes and to use an approximate DFT Hamiltonian to compute the normal modes.^{14,17} This elegant and balanced approach uses the same Hamiltonian for the calculation of the vibrational modes and the electrical transport properties; its main disadvantage (at the moment) is that the computed frequencies are generally worse than those computed with conventional quantum chemical methods and scaling factors are (yet) unavailable. The quantum chemical study of large clusters containing many metal atoms and a molecule is relatively new, and several unsolved issues make it particularly problematic: there are many quasi-degenerate orbitals around the Fermi level which make the SCF wavefunction very unstable with respect to the small geometry alterations (it is necessary to study the variation of the wavefunction with the nuclear coordinates to simulate IETS).

Theoretical and computational studies can provide an accurate and efficient predictive method, but also can help build an intuitive understanding of the technique so that structure/function relations can be developed and experiments understood. One approach toward this is to develop simplified models that are checked against the experimental and the computational results. Accordingly, we have exploited the concept of tunneling path, and a few model systems, to propose a set of propensity rules to be used in the interpretation of IETS spectra.²² Another use of computations to explore the capability and the sensitivity of IETS is to compare simulations of one junction under different conditions (geometry, temperature) to understand which parameters affect the experimental results and how. For example, in a recent paper Kula *et al.* considered the role of the distance between the endgroup and the electrode.²³

Here, we use the model developed by us (normal mode expansion of the transmittance) to investigate the effect of molecular orientation on the IETS spectra of alkane monothiolates. Computing the spectra for different molecular orientations establishes whether the molecular orientation can be deduced from the IETS and which molecular vibrations give signals that are more strongly dependent on the orientation. Alkane monothiolates are a particularly important class for such investigations, since most of the highly ordered SAMs, contain, in fact, an alkylic portion (hydrophobic interactions are one of the driving forces for the SAM formation) and the orientation dependence of IETS of the alkylic group can be used to infer the orientation for SAMs from IETS measurements. We will illustrate our result using a

relatively small molecule (pentane monothiolate) in the all-*trans* conformation. This is not to reduce the computational cost (we have shown that such calculations are computationally very affordable also for much larger systems²⁴) but to simplify the normal mode analysis: this molecule, in fact, displays all the characteristic vibrational modes of the alkane thiol series and it is sufficiently long that none of its atomic orbitals can be strongly coupled to both electrodes.

2. Method

Theory of IETS

Given a molecule sandwiched between two electrodes, it is natural to partition the total Hamiltonian in the three subspaces (left (L) and right (R) electrodes, and molecule (M)), separating the total Hamiltonian into its independent components H^L , H^R , H^M and their interaction V^{LM} , V^{RM} :

$$H = H^L + H^R + H^M + V^{LM} + V^{RM}. \quad (1)$$

The elastic conductance at zero bias can be written as:²⁵

$$g^{\text{el}}(E_F) = g_0 \text{Tr}(\Gamma^L(E_F) \mathbf{G}(E_F) \mathbf{I}^R(E_F) \mathbf{G}(E_F)^\dagger) \quad (2)$$

$g_0 = 2e^2/h$ is the quantum of conductance, Tr indicate the trace operator, E_F is the Fermi level, \mathbf{G} is the reduced Green's function matrix associated with the retarded Green's function operator

$$G(E) = (E - H - i\epsilon)^{-1}_{\epsilon \rightarrow 0}; \quad (3)$$

the matrices Γ^L and \mathbf{I}^R are twice the imaginary part of the self energy and they describe the molecular levels broadening due to the interaction with the metal. For example Γ^L is defined as

$$\Gamma_{ij}^L(E) = 2\pi \sum_l V_{il}^{LM*} V_{lj}^{LM} \delta(E - E_l) \quad (4)$$

where l is a summation index over the states on the left electrode (eigenstates of the isolated electrode) and V_{il}^{LM} or V_{lj}^{LM} is the coupling between these and the orbitals on the molecule (indexes i and j). The imaginary component of the self-energy incorporates information on the density of states of the metal and the coupling between the metal and the molecule. An approximate form for the computation of Γ^L is given by

$$\Gamma_{ij}^L(E) = 2\pi \sum_k V_{ik}^{LM*} V_{kj}^{LM} \text{LDOS}(E)_k \quad (5)$$

where $\text{LDOS}(E)_k$ is the local density of states on the atomic orbital k of the electrode surface and the summation is extended to all atomic orbitals with non negligible coupling with the molecule (all the quantities in eqn (5) are easily accessible from quantum chemical computations).

$G(E)$, like the Hamiltonian, depends parametrically on the nuclear coordinates of the molecule. Given the set of dimensionless normal modes $\{Q_\alpha\}$, it is possible to define the matrices \mathbf{G}^α (one for each normal mode α) whose matrix elements are:

$$G_{ij}^\alpha = \frac{\sqrt{2}}{2} \left(\frac{\partial G_{ij}(E, \{Q_\alpha\})}{\partial Q_\alpha} \right)_{\{Q_\alpha\}=0}. \quad (6)$$

It can be shown that each vibrational mode α contributes to the IETS with a vibrational peak at energy $\hbar\omega_\alpha$ (and voltage $V = \hbar\omega_\alpha/e$), whose intensity is given by:¹⁰

$$W_\alpha = g_0 \text{Tr}(\Gamma^L(E_F) \mathbf{G}^\alpha(E_F) \Gamma^R(E_F) \mathbf{G}^\alpha(E_F)^+). \quad (7)$$

This equation is valid if the E_F is far from any electronic level of the molecule and the elastic conductance is consequently much smaller than g_0 (these are also the conditions required to *measure* a good IET spectrum). When eqn (7) is not valid, other effects (like polaron transport) dominate the I/V characteristic and the IETS is not measurable.²

Several effects contribute to the homogeneous broadening,^{19,26} that will define the appearance of the spectrum (together with inhomogeneous broadening). As is customary in computational spectroscopic studies, the broadening is set to a single empirical value for all signals to help the comparison between experimental and theoretical spectra. It is useful to plot the IETS as $(d^2I/d^2V)/(dI/dV)$ versus V , so that the areas under the IETS peaks are dimensionless values corresponding to the ratio $W_\alpha/g(E_F)$. The details of the formalism outlined above are given in ref. 10 while the details of the implementation used in the present paper are given in ref. 27.

Normal modes computation

To study the orientation dependence of IET spectra it is more convenient first to optimize and compute the vibrational frequencies of the isolated molecule; the optimized structure and normal modes can then be translated into the junction geometry for any given molecular orientation. Quantum chemical calculations can be used to estimate the geometry of the molecule–electrode interface (*e.g.* sulfur–gold distance in small model compounds) but they are ineffective in determining the orientation of the molecule in the junction because this is largely determined by the interaction with other molecules in the monolayer and by the motions of the gold atoms. Since we want to analyze the dependence of the IET spectra of alkane monothiolates on the orientation of the molecule, we must assume that the interaction among molecules determines the orientation without affecting substantially the molecular normal modes (this is a good assumption, since these interactions are of weak van der Waals type and considering the similarity of Raman spectra in solid and solution). We will therefore set a particular molecular orientation and we will rotate the molecular normal modes computed in a vacuum into the preset geometry. The molecular optimization and frequency calculation were performed at the B3LYP/6-31G* level including the terminal hydrogen on the thiol group.

Junction geometry

The sulfur atom of the thiolate is placed on the fcc site of the Au(111) surface with an Au–S distance of 2.86 Å (determined by cluster calculations²⁷). The interaction of the methyl termination with gold is weaker and more difficult to determine using cluster calculations. We consider a Au(111) surface parallel to the other electrode. In the calculations presented here, the carbon of the terminal methyl group is at a distance of 3.51 Å from the gold surface and positioned in correspondence of the bridge site (*i.e.* between two gold atoms) of the

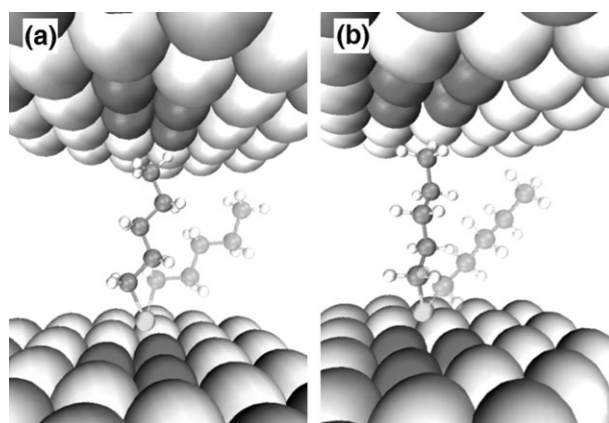


Fig. 1 Pentane monothiolate sandwiched between two electrodes in the perpendicular orientation and in the orientations tilted 40° (in lighter color). The molecule is tilted (a) in the plane containing the carbon atoms, or (b) in the plane perpendicular to the plane containing the carbon atoms. The 3 and 4 darker gold atoms of the bottom (left) and top (right) electrodes are the ones explicitly included in the computation of the self-energy (the top electrode is shown in the geometry of the perpendicular orientation).

gold surface. We observed that, for a given distance between the methyl carbon and the surface, the exact position of the methyl group with respect to the gold surface does not affect the computed IET spectrum. This is probably due to the absence of a specific chemical bond between the methyl and the gold surface (the large dimension of the 6s gold orbital makes the coupling with the molecule at 3.51 Å quite insensitive to the interaction site). The tilt of the molecule is defined by the angle formed by the normal to the electrode connected to the sulfur and the vector connecting the sulfur atom and the carbon of the terminal methyl group. We considered the cases of the molecule tilted in the plane containing the carbon chain and the molecule tilted in the perpendicular plane (see Fig. 1).

Self-energy and IETS computation

For each orientation the normal modes are assumed to be the same, but the self-energy and \mathbf{G}^α are different and they need to be recomputed. The procedure can be summarized as follows:

(i) Two clusters are built, the first containing only the molecule and the few atoms of the left electrode (say the ones connected through the sulfur) and the second containing the molecules and few atoms of the right electrode (the ones in contact with the methyl group). From the single point calculation of these clusters, the electronic couplings between atomic orbitals on the molecule and on the electrode (V_{ij}) are derived. Only singlet state calculations have been performed so that 3 and 4 gold atoms have been included in the cluster with the left and right electrode (they are illustrated in Fig. 1).

(ii) The self-energy is computed from the matrix elements V_{ij} and the local density of states on the gold surface, which was derived from a tight binding calculation of a very large gold cluster. The details of the self-energy calculation are identical to those described in ref. 27. Differently from our first applications of the model,^{10,11} each electrode interacts with many atomic orbitals of the molecules (not only its closest neighbors).

(iii) The Green's function derivative of eqn (6) needs to be computed for each mode, for each orientation (the self-energy in G is orientation dependent). The intensity of the inelastic peaks is computed from eqn (7). The numerical derivation was performed using a displacement of 0.05 adimensional units. The component of the normal modes concerning the displacement of the hydrogen in the thiol group was disregarded.

3. Results

Broadened spectrum

Fig. 2 shows the broadened spectrum for the molecule in the orientation perpendicular to the electrode and tilted 10° , 20° , 30° , 40° in two perpendicular directions. The Gaussian broadening was set to 80 cm^{-1} (an empirically chosen value) for all the spectra and the low energy region of the experimental spectra is also reproduced in Fig. 2. The peak intensities, from which these spectra are plotted, are presented in Table 1. We first discuss the overall appearance of the spectrum and therefore its individual contributions. Apart from the signal associated with the C–H stretching at 3000 cm^{-1} , the experimental spectrum displays three features peaked at ~ 700 , ~ 1050 and

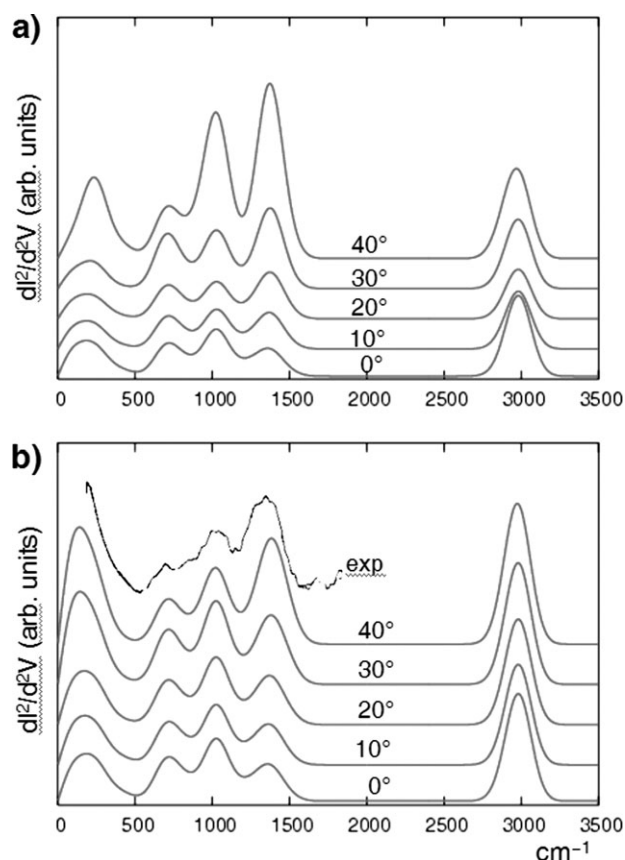


Fig. 2 Simulated IET spectrum of the alkyl monothiolate as a function of the tilting angle with respect to the normal to the surface. Molecule is tilted in the plane of the carbon chain (a) or in the plane perpendicular to the carbon chain (b), as illustrated in Fig. 1. In (b) the experimental spectrum of ref. 7 is shown to illustrate the greater agreement obtained in the case of tilted geometries. Spectra are scaled and shifted vertically for clarity.

Table 1 Computed absolute IETS intensities for the most important normal modes. The dimensionless intensity $1000 \times W_\alpha/g(E_F)$ is reported

N	Freq. ^a	Tilting angle		
		0°	40° ^b	40° ^b
1	63.92	4.4	6.5	16.9
2	97.66	2.1	2.5	10.7
3	113.07	10.2	9.7	14.7
4	143.50	0.4	0.4	11.0
6	238.24	16.3	78.5	20.9
7	243.12	0.3	4.4	6.8
8	334.76	1.9	3.9	2.7
9	422.53	3.1	11.9	1.5
10	708.02	19.4	51.8	19.3
14	839.12	6.8	9.1	3.2
15	882.73	1.1	16.6	2.8
17	996.41	1.4	16.3	6.9
18	1029.08	24.3	69.6	16.2
19	1036.43	3.0	68.1	11.8
21	1107.31	2.6	8.0	2.8
23	1221.78	5.4	5.5	3.7
28	1348.47	5.5	22.1	3.6
29	1376.89	4.9	133.0	30.1
30	1395.44	5.4	24.7	7.3
32	1465.28	0.1	3.1	2.1
33	1468.45	1.3	12.4	5.8
34	1478.43	0.6	3.9	5.8
38	2912.86	2.4	26.9	4.5
42	2937.63	5.2	2.2	5.5
43	2956.45	0.0	0.2	3.3
46	2999.82	0.1	1.5	13.8
47	3005.15	47.6	77.3	41.1

^a Computed frequencies are scaled by the recommended factor 0.965. ^b Geometries corresponding to the two tilting directions of Fig. 1.

$\sim 1350\text{ cm}^{-1}$ and of increasing intensity. The simulated spectrum displays the same three features but their relative intensity is dependent on the molecular orientation. With reference to the peak at 700 cm^{-1} , the peak at 1050 cm^{-1} doubles its intensity when the molecule is tilted 40° in the plane of the C–C backbone while the peak at 1350 cm^{-1} shows a 4-fold increase of its relative intensity for the same tilting. The relative intensities of the three peaks match the experimental pattern for the most tilted orientation considered. The effect is very similar when the tilting in the perpendicular plane is considered (Fig. 2b). Experimentally, the tilting angle for SAM of alkanes (both directions of tilting are in the SAM) increases with the length of the molecule²⁸ and the value expected for the molecule used experimentally is 35° . From an initial overview of these results, it seems evident that the IETS is predicted to be sensitive to the molecular orientation.

Detailed normal mode analysis

Many vibrations contribute to the IET spectrum and the normal mode analysis can be particularly tedious for larger molecules. We can take advantage of considering a relatively small molecule and we analyze each of the normal modes that contribute to the observed features of the broadened spectrum. We number the normal modes from the lowest to the highest energy mode.²⁹ Fig. 3 shows the computed intensities of the IETS with tilting angle 0° and 40° in the plane of the carbon

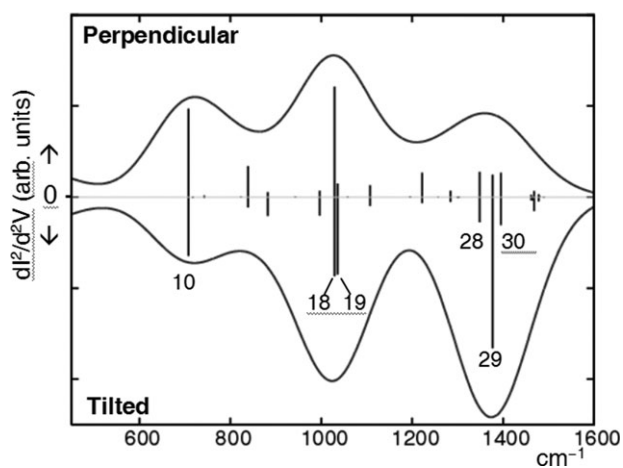


Fig. 3 Comparison between the computed IET spectrum of the pentane monothiolate in the perpendicular orientation (top half of the figure) and the orientation tilted 40° in the molecular plane (mirrored in the bottom half of the figure). The different shape can be attributed to different relative intensity of modes 19 and 29.

backbone, with labels indicating the most important vibrations. The results (and the following discussion) are identical if the other direction of tilting is considered, as it can be seen from Table 1, which contains the results for all tilting angles in more detail. Fig. 4 displays the most important normal modes labeled as in Fig. 3. The feature at 700 cm^{-1} is due to the C–S stretching mode, the feature at 1050 cm^{-1} is due to several C–C stretching modes (with an important component of the CH_2 wagging modes) and the feature at 1350 cm^{-1} is due to the CH_2 wagging modes (with an important component of the C–C stretching modes).

The relative intensity increase of the broadened peaks at 1000 cm^{-1} and 1350 cm^{-1} is due to just two vibrations, 19 and 29, which increases their relative importance when the molecule is tilted. These two normal modes are very similar: they

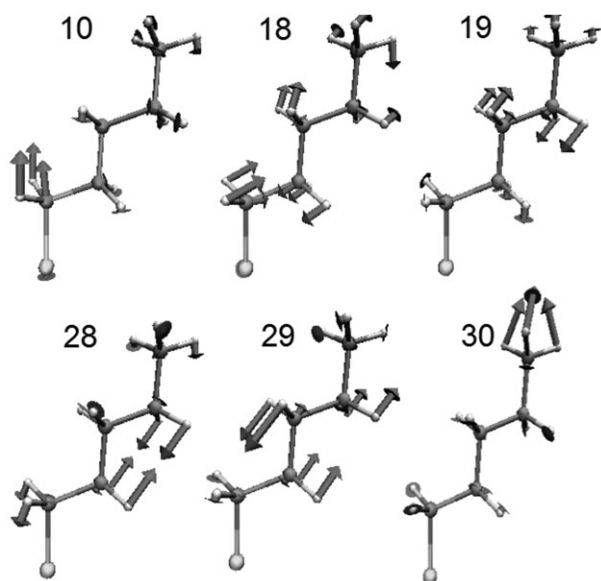


Fig. 4 Selected normal modes of pentane monothiol (labeled as in Fig. 3).

contain an ‘antisymmetric’ stretching combination of the bonds C2–C3 and C3–C4 mixed with a CH_2 wagging mode (the two linear combinations of stretching and wagging have different signs and the wagging dominates mode 29 while the stretching dominates mode 19).

Interpretation in terms of tunneling paths

In a theoretical analysis focused on conjugated molecules of C_{2h} symmetry, we showed that one can rationalize the result of the quantum chemical computation of IETS using the concept of tunneling paths and some symmetry considerations. A tunneling path³⁰ is a series of adjacent atomic orbitals that mediate efficiently the coupling between the two electrodes. Typically, for any molecule there are few active tunneling paths that can be identified intuitively or by analyzing the numerical results. For alkyl chains the tunneling path invariably involves a σ bonding orbital of the carbon backbone. The most effective vibrations in IETS are those that modulate the coupling along the most favorable tunneling path.²² In this case, a normal mode can be IETS active only if it contains a fair amount of C–C stretching. However, not all the vibrations that contain C–C stretching are IETS active, because the relevant matrix elements can be null by symmetry. For alkane monothiolates the only symmetry element (in vacuum) is the plane of the carbon atoms and the only propensity rule that can be obtained is that a' (in plane) vibrations are active and a'' (out of plane) vibrations are inactive in IETS. This rule is perfectly obeyed in this case (all peaks visible in Fig. 3 are of a' type and the intensity of the a'' vibrations is numerically zero).

In addition to the rigorous molecular symmetry, there are some other modes that display locally a *quasi-symmetry*³¹ that can be used to interpret their relative intensities (see Fig. 5). Modes 19 and 29 contain a combination of the C₂–C₃ stretching and the C₃–C₄ stretching that can be considered (quasi) antisymmetric with respect to the carbon atom C₃. Of course, the antisymmetry is only approximate since there is no rigorous symmetry element that overlaps the bond C₂–C₃ with the bond C₃–C₄. According to the symmetry rule given in ref. 21, an antisymmetric vibration involving three consecutive atoms

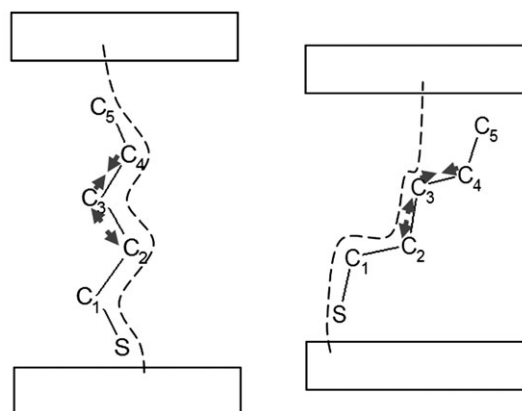


Fig. 5 Pentane monothiolate in the perpendicular (left) and tilted (right) orientation. The small arrows indicate the asymmetric stretching present in modes 19 and 29. The dashed line helps visualizing the most important tunneling paths: the path avoiding C₄ and C₅ increases its importance in the tilted orientation.

should not contribute to the IET spectrum if the main tunneling path involves these three atoms. A simple geometric consideration outlined on the idealized chart below suggests that, when the molecule is perpendicular to the surface, all electrons will tunnel through the molecule and the tunneling path will always involve the C₂–C₃–C₄ triad. The (quasi) antisymmetric combination of their stretching will be (quasi) forbidden, *i.e.* modes 19 and 29 will be weak. However, as the molecule is tilted, the direct coupling of the C3 atom with the electrode is much increased and the probability of a tunneling path Gold–C₃–C₂–C₁–S–Gold can become competitive with the path Gold–C₅–C₄–C₃–C₂–C₁–S–Gold (the argument does not change if we include the effect of hydrogen atoms). A quantitative model is given in the next subsection, where it is shown that the importance of the shorter path can be similar to that of the longer path for a reasonable set of parameters and sufficient tilting. For the short tunneling path, modes 19 and 29 are not forbidden because this path does not involve atom C₄. We can therefore interpret the increase of the relative intensities of modes 19 and 29 as an effect of the additional short tunneling path, which increases its importance as the tilting angle increases.

Simple model for the bypassing of terminal groups in tilted linear chains

To verify that the bypassing of the terminal groups is not unexpected on the basis of experimental data on electron tunneling, we consider the following simplified model: a linear chain of N atoms, between two electrodes, tilted by an angle θ with respect to the normal to the electrodes. Each atom has only one orbital and the distance between atoms is d . Indicating with g_{ij} the (zero bias and elastic) conductance if only the atoms i and j were coupled to the electrode, we write the conductance g_{1N} and $g_{1,N-2}$ as:

$$g_{1N} = |G_{1N}|^2 \Gamma_{11}^L \Gamma_{NN}^R, \quad (8a)$$

$$g_{1,N-2} = |G_{1,N-2}|^2 \Gamma_{11}^L \Gamma_{N-2,N-2}^R. \quad (8b)$$

g_{1N} and $g_{1,N-2}$ correspond to the conductance in the two tunneling paths indicated in Fig. 6 (an idealization of the situation described in Fig. 5).

We can now estimate the relative importance of the shorter tunneling path evaluating the ratio $g_{1,N-2}/g_{1N}$. $\Gamma_{N-2,N-2}^R$ is smaller than Γ_{NN}^R because of the larger distance from electrode and the consequently reduced coupling. Numerous experiments on the distance dependence of tunneling through a vacuum (*e.g.* STM experiments) indicate that the tunneling

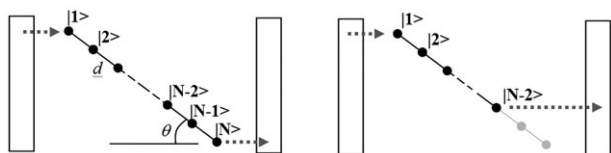


Fig. 6 The tunneling path through the whole molecule, related to the conductance g_{1N} (left). The tunneling path bypassing the terminal atoms, related to the conductance $g_{1,N-2}$ (right).

current decreases exponentially with distance, so that we can write

$$\Gamma_{N-2,N-2}^R = \Gamma_{NN}^R \exp(-\alpha(2d)\cos\theta). \quad (9)$$

Here α is the exponential fall off parameter of the tunneling current. $|G_{1N}|^2$ is smaller than $|G_{1,N-2}|^2$ because it is related to the effective coupling through a longer tunneling path. It is simple to show³² that, for a linear chain in the Landauer–Imry regime (far below the voltage needed for electronic resonance), $|G_{1N}|^2$ decreases exponentially with the length of the chain. Measuring the electron transfer rate constant in donor–bridge–acceptor systems as a function of the bridge length, it was experimentally observed that $k^{\text{CT}} = k^0 \exp(-\beta \cdot R_{\text{DA}})$, with R_{DA} the distance between donor and acceptor. Since the charge transport rate in a bridge mediated electron tunneling is proportional to $|G_{1N}|^2$ we can write:³³

$$|G_{1N}|^2 = |G_{1,N-2}|^2 \exp(-\beta \cdot 2d) \quad (10)$$

and we can therefore evaluate the ratio $g_{1,N-2}/g_{1N}$ as

$$\frac{g_{1,N-2}}{g_{1N}} = \exp \left[2\beta d \left(1 - \frac{\alpha}{\beta} \cos\theta \right) \right] \quad (11)$$

Since $\alpha > \beta$ (the distance dependence of the tunneling probability is stronger in vacuum), the longer path across the molecule (1, N) is always more favorable than the short path (1, $N-2$) when the molecule is perpendicular ($\theta = 0$). The two paths become of equivalent importance when $\theta = \theta^0 = \arccos(\beta/\alpha)$.

From literature we can take $\beta \sim 1 \text{ \AA}^{-1}$ (for saturated bridges) and ($\alpha \sim 2.3 \text{ \AA}^{-1}$) in vacuum.³² These parameters imply that $\theta^0 \sim 64^\circ$ and that the ratio $g_{1,N-2}/g_{1N}$ increases by a factor of 3 when θ increases from 0° to 40° (using an ‘effective’ $d = 1 \text{ \AA}$). This is in very good agreement with the increase of the IETS intensity of the modes 19 and 29 that we attributed in the last subsection to an increased importance of the ‘short’ tunneling path.

We note that the possibility of the electron tunneling through a smaller portion of the molecule (and a larger portion of vacuum) is probably limited to saturated molecules. For conjugated species, β is typically much smaller and, for any reasonable tilting angle, the through molecule path is always much more favorable.

4. Conclusion

We used a computational model for simulating IETS to show that the spectra of alkane monothiolates is dependent on the orientation of the molecule in the junction. Three main peaks dominate the experimental IET spectrum in the 500–1700 cm^{-1} range and they are well reproduced by the simulations. However, the relative intensity of these peaks is reproduced correctly only if the molecule is tilted by 30° – 40° with respect to the surface normal (corresponding to the orientation determined by other experimental techniques).

This observation can be important to maximize the amount of information retrievable from IET measurements, since we can expect to observe similar orientation dependence for other systems and the comparison between simulation and

experiment can be used to infer the correct orientation when no other experimental data are available. Moreover, alkyl termination is very common in SAM monolayers, so that the current results can be used to determine the orientation in different SAM junctions characterized by the contact between an alkyl fragment and the gold electrode.

The origin of the orientation dependence in alkanes was investigated using the intuitive framework of tunneling path analysis. Two normal modes of the considered molecule increase their relative intensity as the molecule is tilted. Both modes contain an asymmetric C–C–C stretching combination which is IETS-forbidden for the tunneling path crossing the whole carbon backbone of the molecule, but is IETS-allowed for the tunneling path that bypasses the last two carbon atoms of the molecule. This tunneling path through a smaller portion of the molecule is not very important for the perpendicular orientation but its role increases as the molecule is tilted because the electrode is effectively coupled to more carbon atoms of the molecule (not just the terminal one). Using a simple model based on well known data from tunneling literature we showed that this interpretation is consistent with the computed spectra.

An important suggestion deriving from this analysis is that the tunneling path idea is very useful for interpreting the IETS measurements and that IETS can provide more experimental evidence of the tunneling path concept, which has been used by theoreticians in the past 15 years without the possibility of a direct verification.

Acknowledgements

This work was supported by the Royal Society (UK), DARPA Mol Apps, DOD MURI program, NASA URETI program, NSF International Division.

References

- 1 *Introducing Molecular Electronics: A Brief Overview, Lecture Notes in Physics*, ed. G. Cuniberti, G. Fagas and K. E. Richter, Springer, Berlin, 2005, vol. 680.
- 2 A. Troisi and M. A. Ratner, *Small*, 2006, **2**, 172.
- 3 R. C. Jaklevic and J. Lambe, *Phys. Rev. Lett.*, 1966, **17**, 1139.
- 4 K. W. Hipps and U. Mazur, *J. Phys. Chem.*, 1993, **97**, 7803.
- 5 B. C. Stipe, M. A. Rezaei and W. Ho, *Science*, 1998, **280**, 1732.
- 6 W. Y. Wang, T. Lee, I. Kretzschmar and M. A. Reed, *Nano Lett.*, 2004, **4**, 643.
- 7 J. G. Kushmerick, J. Lazorcik, C. H. Patterson, R. Shashidhar, D. S. Seferos and G. C. Bazan, *Nano Lett.*, 2004, **4**, 639.
- 8 N. Mingo and K. Makoshi, *Phys. Rev. Lett.*, 2000, **84**, 3694.
- 9 N. Lorente, M. Persson, L. J. Lauhon and W. Ho, *Phys. Rev. Lett.*, 2001, **86**, 2593.
- 10 A. Troisi, M. A. Ratner and A. Nitzan, *J. Chem. Phys.*, 2003, **118**, 6072.
- 11 A. Troisi and M. A. Ratner, *Phys. Rev. B: Condens. Matter*, 2005, **72**, 033408.
- 12 D. P. Long, J. L. Lazorcik, B. A. Mantooth, M. H. Moore, M. A. Ratner, A. Troisi, Y. Yao, J. W. Ciszek, J. M. Tour and R. Shashidhar, *Nat. Mater.*, 2006, **5**, 901.
- 13 J. Jiang, M. Kula, W. Lu and Y. Luo, *Nano Lett.*, 2005, **5**, 1551.
- 14 M. Paulsson, T. Frederiksen and M. Brandbyge, *Nano Lett.*, 2006, **6**, 258.
- 15 Y. C. Chen, M. Zwolak and M. Di Ventra, *Nano Lett.*, 2005, **5**, 621.
- 16 N. Sergueev, D. Roubtsov and H. Guo, *Phys. Rev. Lett.*, 2005, **95**.
- 17 G. C. Solomon, A. Gagliardi, A. Pecchia, T. Frauenheim, A. Di Carlo, J. R. Reimers and N. S. Hush, *J. Chem. Phys.*, 2006, **124**, 094704.
- 18 A. Pecchia and A. Di Carlo, *Nano Lett.*, 2004, **4**, 2109.
- 19 M. Galperin, M. A. Ratner and A. Nitzan, *J. Chem. Phys.*, 2004, **121**, 11965.
- 20 Y. Asai, *Phys. Rev. Lett.*, 2004, **93**.
- 21 It should be noted that high resolution spectroscopies used to retrieve information about a chemical system usually operate in the linear response regime, *i.e.* the perturbation is small enough that the response gives information about the system and not about the system plus the perturbation. IETS is a very useful technique when the perturbation is sufficiently small to be treated within the perturbative theory.
- 22 A. Troisi and M. A. Ratner, *Nano Lett.*, 2006, **6**, 1784.
- 23 M. Kula, J. Jiang and Y. Luo, *Nano Lett.*, 2006, **6**, 1693.
- 24 A. Troisi and M. A. Ratner, *Phys. Rev. B: Condens. Matter*, 2005, **72**, 0333408.
- 25 A. Nitzan and M. A. Ratner, *Science*, 2003, **300**, 1384.
- 26 A. Nitzan, *Nano Lett.*, 2004, **4**, 1605.
- 27 A. Troisi and M. A. Ratner, *J. Chem. Phys.*, 2006, **125**, 214709.
- 28 P. Fenter, A. Eberhardt, K. S. Liang and P. Eisenberger, *J. Chem. Phys.*, 1997, **106**, 1600.
- 29 A rigorous normal mode numbering is not available because (i) the symmetry of the molecule in vacuum can be lowered by the interaction with the surface (ii) the classification of the IR and Raman spectra is performed for the molecule with the hydrogen attached to the sulfur atom (and this alters completely the normal mode numbering). We used here the simplest possible choice (assigning mode numbering based simply on increasing frequency) with the aim of making these results easily comprehensible.
- 30 D. N. Beratan, J. N. Betts and J. N. Onuchic, *Science*, 1991, **252**, 1285.
- 31 H. Zaborodsky, S. Peleg and D. Avnir, *J. Am. Chem. Soc.*, 1992, **114**, 7843.
- 32 A. Nitzan, *Chemical Dynamics in Condensed Phases*, Oxford University Press, New York, 2006.
- 33 The coefficients α and β are expected to depend weakly on the injection energy.